Voltage Stability Probabilistic Assessment in Composite Systems: Modeling Unsolvability and Controllability Loss

Anselmo Barbosa Rodrigues, Ricardo B. Prada, and Maria Da Guia da Silva, *Member, IEEE*

***Abstract*—Several papers have recognized the effect of uncertainties in voltage stability analysis through probabilistic methods. In these papers, the unstable states are generally identified by the unsolvability of the power flow equations or by violations in the voltage stability margin limit. However, voltage stability problems may also be associated with a loss in voltage controllability, when a voltage control action has an effect which is contrary to what is usually expected. The main aim of this paper is to include unstable states caused by unsolvability and voltage controllability loss in the voltage stability probabilistic assessment. This goal is achieved through the combination of three techniques: the Monte Carlo Simulation Method, the nonlinear optimal power flow and the D' matrix method. These three techniques permit the inclusion of a new issue in the computation of voltage instability risk: the unstable states stemming from controllability loss.**

***Index Terms*—Composite systems, interior point method, Monte Carlo simulation, optimal power flow, probabilistic methods, sensitivity analysis, voltage stability.**

List of Acronyms

BTS-65	Brazilian Test System of 65 buses.
BTS-107	Brazilian Test System of 107 buses.
C	Circuit contingencies (lines and transformers).
DMM	D' Matrix Method.
G	Generator and compensator outages.
GC	Simultaneous failures in circuits and generators.
L	Fluctuations in the system peak load due to forecasting errors (without equipment in down state).
LOLP	Loss of load probability.
MCSM	Monte Carlo Simulation Method.
MRTS	Modified version of the IEEE Reliability Test System.
NI	Number of islands.
NS^{max}	Maximum number of simulations for the MCSM.
OPF	Optimal power flow.
P (Health)	Health state probability.
P (Marginal)	Marginal state probability.
P (Emergency)	Emergency state probability.
P (Collapse)	Collapse state probability.
SLP	Sequential linear programming.
SQP	Sequential quadratic programming.
SRPFE	Solvability restoration of the power flow equations.
VIR	Voltage instability risk.
VSM	Voltage stability margin.
VSPA	Voltage stability probabilistic assessment.

Manuscript received May 29, 2009; revised August 21, 2009. First published January 26, 2010; current version published July 21, 2010. This work was supported in part by FAPEMA (Fundação de Amparo à Pesquisa e ao Desenvolvimento Científico e Tecnológico do Estado do Maranhão), in part by ELETRONORTE (Centrais Elétricas do Norte do Brasil S.A), and in part by CNPq (Conselho Nacional de Desenvolvimento Científico e Tecnológica). Paper no. TPWRS-00394-2009.

A. B. Rodrigues and R. B. Prada are with the Department of Electrical Engineering, Pontifical Catholic University of Rio de Janeiro, Rio de Janeiro, RJ, Brazil (e-mail: anselmo@ele.puc-rio.br; prada@ele.puc-rio.br).

M. G. da Silva is with the Department of Electrical Engineering, Federal University of Maranhão, São Luís, MA, Brazil (e-mail: guia@dee.ufma.br).

Digital Object Identifier 10.1109/TPWRS.2009.2039234

I. Introduction

CURRENTLY, electric power systems are operating near to their limits. This operational condition has been caused by the following factors: the natural growth of demand for electric energy and postponement in transmission expansion caused by routing constraints and reductions in the electricity sector budget due to economic difficulties. The operation of heavily loaded transmission lines has given rise to voltage stability problems in electricity networks. Voltage stability is defined as the ability of a power system to maintain steady voltages at all the buses after disturbances such as: load fluctuations and contingencies in the system components [1], [2]. The voltage instability states are mainly associated with two mechanisms:

1) **Unsolvability of the power flow equations [3], [4]:** after the occurrence of a system disturbance, the power flow equations do not have real solutions due to the violation in the limit of maximum power transfer for the system loads. The distance between the current loading point and the maximum loading point is denominated as VSM.

2) **Voltage controllability loss [1], [5]:** after a disturbance, the control actions, used to correct the voltage profile, have the opposite effect to that which is expected. For example, voltage reduction in a bus after a capacitor bank is switched on. This effect is due to the negative value of the QV sensitivity in the bus where the capacitor was switched on.

The presence of the voltage instability mechanisms in a system state can be identified through the combination of the following techniques:

1) DMM [5] or modal analysis [6] to detect controllability loss problems;
2) OPF [4] or continuation power flow [7] to assess the solvability of the power flow equations.

This identification can be carried out due to voltage instability mechanisms rely on the existence of real solutions for the power flow equations and on the sensitivity relationships between control and state variables. However, it is not possible to predict the system operational state. It is due to the stochastic behavior of load fluctuations and equipment availability. Consequently, the system is subject to an uncertainty associated with the occurrence of voltage instability states. Therefore, it is important that the voltage stability analysis should also consider the uncertainties related to random nature of system disturbances. Due to this, the more appropriate techniques for modeling uncertainties associated with system disturbances in voltage stability are the probabilistic methods. The main advantages of the probabilistic methods are their ability to combine severity and likelihood to truly express the system risk [8], [9]. Furthermore, several disturbances caused by voltage instability problems have been reported in the literature [2], [5]. These events have motivated the development of tools to quantify the VIR. This interest in evaluating the VIR has resulted in several papers related to VSPA [10]–[16].

In [10], the nonlinear OPF [4] and the MCSM are combined to assess the impact of the voltage instability problems on the reliability indices based on load curtailments. The nonlinear OPF was used to evaluate the amount of load curtailment required to restore the solvability of the power flow equations. Consequently, all solvable states are considered as stable states. Due to this, the method proposed in [10] cannot identify voltage instability problems caused by controllability loss.

An approach for carrying out a reliability evaluation of bulk power systems with voltage stability constraints is proposed in [11]. This approach is based on the combination of the Bisection Method with the L index [17]. The Bisection Method is used to determine the load curtailment necessary to satisfy a target value for the VSM estimated by the L index. Nevertheless, the L index can estimate the VSM only for load buses. However, voltage instability problems caused by controllability loss occur more frequently in buses with reactive power generation [5]. Due to this, the L index cannot accurately identify voltage instability states caused by controllability loss problems.

In [12], the impact of voltage stability constraints on the reliability indices is assessed using a linear OPF model and voltage limit curves. These curves are obtained for a critical contingency list which refers to voltage stability problems. If a selected contingency in the adequacy assessment belongs to a critical contingency list then the voltage stability operation curves for this contingency are converted in linear constraints. Then, these linear constraints are added to the linear OPF used to simulate corrective actions. The main problem with this approach is that unstable states are deterministically selected. That is, unstable states associated with noncritical contingencies cannot be identified. It is because the adequacy assessment of a sampled state is carried out without considering voltage and reactive issues. That is, the nonlinear nature of the voltage stability phenomena is ignored for noncritical contingencies.

The VIR for the system and load buses is evaluated in [13]. In this paper, the L index is again used to identify voltage instability states based on a threshold for the VSM. Consequently, the indices evaluated in [13] have the same problems of those obtained in [11].

In [14], an approach is proposed for evaluating the VIR and the expected VSM considering uncertainties associated with the load forecasting error. These probabilistic indices have been estimated using two techniques: the MCSM and the Tangent Vector Method [18]. An important contribution of [14] is the evaluation of VSM for a specified risk level. However, the methodology proposed in this reference can be extended to include the following issues in VSPA: 1) the evaluation of VIR index considering unstable states caused by controllability loss problems; 2) the severity assessment of the unsolvable states, that is, the identification of the unsolvable states that can be restored with no load curtailment; and 3) outages in transmission and generation equipments.

A methodology based on the state enumeration method is proposed in [15] to estimate the VIR index. In this paper an unstable state is identified when the difference between the maximum and the current system loadings is the negative. The maximum system loading for each selected state is evaluated using a continuation power flow [7]. Consequently, voltage instability problems associated with power flow unsolvability can be correctly identified. Nevertheless, only four single transmission outages are considered in the computation of the VIR index. Furthermore, the method proposed in [15] does not take two important issues relating to the VSPA index into consideration: voltage instability problems caused by controllability loss and the severity of the unstable states associated with the power flow unsolvability.

Reference [16] presents a method for evaluating reliability indices in composite systems taking voltage instability constraints into consideration. In this paper, voltage stability constraints are embedded in a corrective actions algorithm, based on nonlinear OPF, using the L index. Due to this, the proposed method in [16] cannot exactly assess the effects of controllability loss problems on the reliability indices.

The VSPA carried out in [10]–[16] is oriented to two paradigms:

1) assessment of the impact of voltage stability constraints on the reliability indices [10]–[12], [16];
2) evaluation of the probabilistic indices associated with unstable states [10], [13]–[15].

At this point, it is important to mention that in both paradigms described above, the unstable states are identified using two criteria: unsolvability of the power flow equations or violation of the VSM limit. In other words, the unstable states associated

with controllability loss have not been considered in the VSPA. Nevertheless, controllability loss problems have been reported in several voltage instability incidents, such as the disturbance of the South/South-East Brazilian system on April 24, 1997 [5]. Therefore, the main aim of this paper is to model both the unsolvability and the controllability loss in the VSPA. This model is based on the combination of three techniques:

1) MCSM [8], [9]: to consider uncertainties associated with peak load forecasting errors and equipment unavailability;
2) DMM [5]: to include controllability loss problems in the probabilistic indices associated with unstable states;
3) nonlinear OPF based on the Interior Point Method [4]: to assess unstable states associated with unsolvability of the power flow equations.

It is important to mention that the unstable states associated with the controllability loss can be also identified using the modal analysis [6]. However, the modal analysis has a computational cost bigger than the one associated with the DMM. The disadvantage of the modal analysis is due to the computation of eigenvalues/eigenvectors to assess the voltage stability of a system bus. On the other hand, the DMM requires only backward/forward solutions, with the LU factors of the power flow Jacobian matrix, to carry out a nodal voltage stability analysis. The computational cost is critical issues feature in VSPA since a large number of system states must be assessed to estimate the indices with an acceptable precision. Thus, the DMM was selected to identify controllability loss problems in the proposed method for VSPA.

The combination of these three techniques has been used to generate the following probabilistic indices: VIR index, Well-being States probabilities [19]–[21], buses expected VSM index, the participation factors of the uncertainties, and of the voltage instability mechanisms on the VIR index. These indices have been evaluated by three test systems: two equivalent systems obtained from the Brazilian interconnected power system [22] (STB-65 and STB-107) and a modified version of the IEEE system of 24 buses [23], [24] (MRTS). The tests results with these three systems demonstrate that the voltage controllability loss has significant impact on the probabilistic indices associated with unstable states. Furthermore, the proposed method accurately identified the areas vulnerable to voltage instability problems in the test systems. Finally, it must be mentioned that the main novelty of the proposed methodology is the inclusion of unstable states caused by controllability loss in the VIR index computation. In the literature this issue has not been considered in previous studies on the VSPA.

The paper is organized as follows: Section II describes the proposed method for carrying out the VSPA. Section III presents the two techniques used in the voltage stability analysis: DMM and nonlinear OPF. Section IV establishes the definitions of the proposed indices for the VSPA. The test results are given in Section V. General conclusions are given in Section VI.

II. Methodology

The voltage stability of an electric network is a function of parameters such as: load level, generation patterns and network topology. These parameters are subject to uncertainties associated with load forecasting errors and component outages. In this paper, the uncertainties associated with network parameters have been included in the VSPA through the MCSM. In this method, the probabilistic indices are estimated through the replication of the system's random behavior. This replication is carried out using the probability distributions that model the uncertainties associated with the system components. The main uncertainties considered in the VSPA are: load forecasting errors and lack of availability of equipment. The load forecasting uncertainty can be modeled through a probability distribution whose parameters are evaluated from past experience and future considerations. However, the available historical data is not sufficient to identify the type of distribution associated with the load forecast errors. Due to this, the most common practice is to describe the load uncertainty by a normal distribution [25]. In this way, it is possible to use a Box-Müller generator [9] to sample a system peak load for each system state selected by the MCSM. Thus, the system peak load is sampled as

$$L^i = L^o + L^o \left(\frac{\sigma^o}{100}\right) X^{norm}$$

where

L^i	system peak load for the system state i;
L^o	system peak load for the base—case condition;
σ^o	load forecasting error (standard deviation) expressed as percentage of L^o;
X^{norm}	random number with normal distribution obtained through the Box-Müller generator.

On the other hand, the equipment unavailability was modeled considering that the component outages are independent and represented by a two state model. Consequently, the probability of outage is the forced unavailability. Thus, the state of a component is sampled as [9]:

1) generate a random number X^{unif} with uniform distribution;
2)

$$s_j^i = \begin{cases} 0\,(\text{down state}), & \text{if } 0 \le X^{unif} < U_j \\ 1\,(\text{up state}), & \text{if } U_j \le X^{unif} < 1.0 \end{cases}$$

where

U_j	unavailability of the component j;
s_j^i	state of the component j in the system state i.

The sampling procedure used in this paper can be easily extended to model large scale generation units that operate at reduced capacity states (derated states). The sampling approach for multi-state generators is based on the division of the interval $[0, 1]$ in subintervals whose widths are equal to the derated states probabilities. For example, the state sampling for a generator with two derated states is carried out as follows [9]:

1) generate a random number X^{unif} with uniform distribution;
2) define the state associated with X^{unif}, shown in the equation at the bottom of the next page. $PD1_j$ and $PD2_j$ are

the probabilities of the two derated states associated with generator j.

The states of the components and the load level are combined to define a system state as

$$s^i = \left(s_1^i, s_2^i, \ldots, s_{NC}^i, L^i\right).$$

NC is the number of components and s^i is the ith sampled system state. The sampling approach described above is used to generate a sample of the system states. These states are assessed in accordance with the flowchart showed in Fig. 1. The main steps of the assessment of a system state are explained as follows.

1) **Topological Processing:** identification of connectivity loss problems (islanding) caused by circuit outages. That is, the topological processing checks if the original graph of the electric network was partitioned in disconnected subgraphs (islands). In this paper, the topological processing is carried out using graph transversal techniques such as breadth and depth searches [26].
2) **Load/Generation Dispatch:** evaluation of the power output of the generators of each island subject to the following constraints: active power balance equation and limits to the generators power output. In thermal systems, the dispatch is achieved using a merit order list of the incremental costs associated with the generators. That is, the generation dispatch in a thermal system is the result of the minimization of the production costs. On the other hand, the generation dispatch of hydroelectric systems is carried out through the minimization of the squared Euclidian distance (quadratic deviation) between the generators power output and a specified generation pattern. This pattern is determined in the short term (daily) scheduling of the hydroelectric plants [27]. Along with the dispatch, it may be necessary to carry out load curtailment to eliminate generation deficit in some system states.
3) **Data Compilation for the Power Flow Study:** data preprocessing required for a power analysis of the sampled state. This step is associated with the following tasks: definition of the buses types (PV, PQ, and Vθ), evaluation of the Mvar limits in buses with reactive power generation, elimination of isolated buses and unfeasible islands (islands without load and generation), etc. At this point, it must be mentioned that the data compilation for the power flow analysis defines one slack bus for each island [28], [29]. This approach eliminates the singularity of the Jacobian matrix caused by the connectivity loss of the electric network [30]. Consequently, it is possible to carry out a single power flow analysis for a system state composed of several islands.
4) **Power Flow:** evaluation of the nodal voltages for the sampled state using the Newton–Raphson Algorithm.
5) **Solvability Restoration with Nonlinear OPF:** elimination of nonconvergence cases of the Newton–Raphson Algorithm using a nonlinear OPF. The SRPFE is performed to analyze the severity of the voltage instability states associated with the unsolvability of the power flow equations. This information is very important for the system operators since it permits the identification of whether there are states in which the unsolvability can be eliminated without load curtailment or not.
6) **Voltage Stability Analysis with DMM:** voltage stability assessment of the sampled state using the DMM. The main aim of this step is the identification of unstable states caused by controllability loss problems.

It should be mentioned that the load/generation dispatch in hydroelectric systems is associated with a convex separable quadratic optimization problem. The problem has only one equality constraint (active power balance equation). Consequently, it is possible to apply the economic dispatch algorithm described in [31] to solve the minimum deviation dispatch. It is then necessary to define a fictitious cost function for each power plant. The cost function is given by

$$C_i\left(Pg_i\right) = a_i Pg_i^2 + b_i Pg_i + c_i$$

where

$$\begin{aligned} a_i &= W_i \\ b_i &= -2W_i Pg_i^o \\ c_i &= W_i \left(Pg_i^o\right)^2. \end{aligned}$$

a_i, b_i, and c_i are the coefficients of the cost function associated with the plant i;

$C_i(Pg_i)$, Pg_i, W_i, and Pg_i^o are: the cost function, the output power, the relative weight and the specified generation for the plant i, respectively.

Furthermore, it can be noted that the steps 1)–4) of the APET algorithm are similar to the violations (overloads, overvoltages, undervoltages, etc.) identification process carried out in composite reliability studies [28], [29]. The main difference between reliability and APET algorithms is that the corrective actions simulation (used in reliability studies to evaluate the amount of load curtailment due to violations in operational constraints) is replaced by the voltage stability assessment of a

$$s_j^i = \begin{cases} 0\ (\text{down state}), & \text{if } 0 \le X^{unif} < U_j \\ 2\ (\text{derated state 2}), & \text{if } U_j \le X^{unif} < U_j + PD1_j \\ 3\ (\text{derated state 3}), & \text{if } U_j + PD1_j \le X^{unif} < U_j + PD1_j + PD2_j \\ 1\ (\text{up state}), & \text{if } U_j + PD1_j + PD2_j \le X^{unif} < 1.0 \end{cases}$$

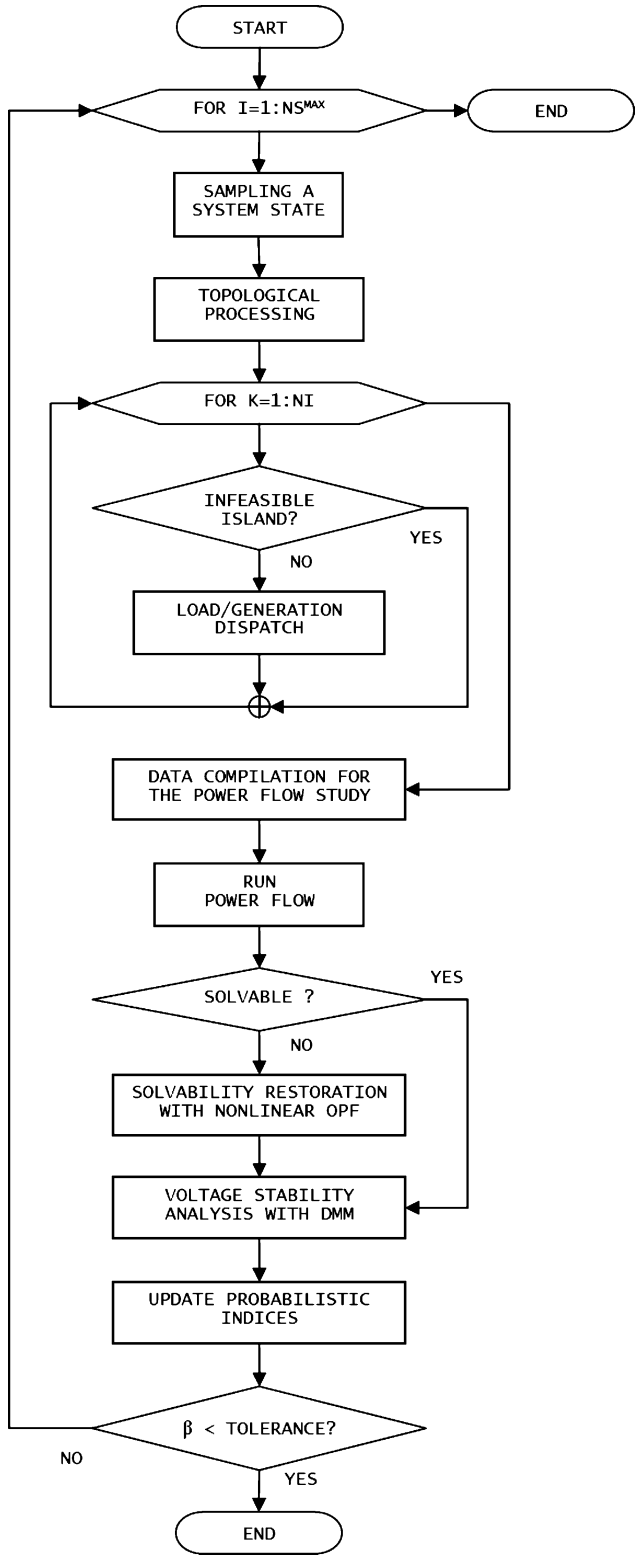

Fig. 1. Flowchart of the proposed method for VSPA.

selected state. In this way, composite reliability programs can be easily expanded to incorporate the APET method proposed in this paper.

The sample of system states assessed with the DMM and by the SRPFE algorithm may be used to estimate probabilistic indices. These indices are evaluated using the sample average definition:

$$\tilde{E}(F) = \frac{1}{NS}\sum_{i=1}^{NS} F(s^i)$$

where

NS inumber of system states;

$\tilde{E}(F)$ mean value of the index F;

$F\left(s^i\right)$ value of the test function associated with the index F in the state s^i. For example, if the estimated index is the LOLP, then $F(s^i) = 1$ when s^i is a failed state (if there is load curtailment in the state s^i), and $F(s^i) = 0$ otherwise.

The uncertainty of the estimate $\tilde{E}(F)$ obtained with the MCSM may be assessed by means of the coefficient of variation [9], [32]. This coefficient is given by

$$\frac{\beta(F) = \tilde{\sigma}(F)}{\tilde{E}(F)}$$

where

$$\tilde{\sigma}(F) = \sqrt{\frac{\tilde{Var}(F)}{NS}}$$

$$\tilde{Var}(F) = \frac{1}{NS-1}\sum_{i=1}^{NS}\left[F\left(s^i\right) - \tilde{E}(F)\right]^2$$

where

$Var(F)$ estimated variance of the index F;

$\tilde{\sigma}(F)$ estimated standard deviation of the index F.

In this paper, the coefficient of variation has been used as a stopping rule for the MCSM. However, the maximum number of simulations is used as safeguard criterion to avoid an inordinate number of simulations being carried out when a specified precision is very small.

III. Voltage Stability of a Sampled State

A. DMM

In this paper the DMM [5] is used to identify whether a state has voltage instability problems caused by the controllability loss. This method is based on the linearized system of the power flow equations:

$$\begin{bmatrix}\Delta P\\ \Delta Q\end{bmatrix} = [J]\begin{bmatrix}\Delta\theta\\ \Delta V\end{bmatrix}. \tag{1}$$

Putting the equations related to the bus i in the bottom of (1):

$$\begin{bmatrix}\Delta P'\\ \Delta Q'\\ \Delta P_i\\ \Delta Q_i\end{bmatrix} = \begin{bmatrix}A & B\\ C & D\end{bmatrix}\begin{bmatrix}\Delta\theta'\\ \Delta V'\\ \Delta\theta_i\\ \Delta V_i\end{bmatrix} \tag{2}$$

where the submatrices A, B, C, and D are originated from a partition of full Jacobian matrix $[J]$. Assuming an incremental variation ΔP and ΔQ only in bus i under analysis ($\Delta P' = \Delta Q' = 0$), it is possible to eliminate the coupling between $[\Delta\theta'\Delta V']$ and $[\Delta\theta_i\Delta V_i]$ through a Kron reduction. Applying this procedure in system (2) it gives

$$\begin{bmatrix} \Delta P_i \\ \Delta Q_i \end{bmatrix} = [D'] \begin{bmatrix} \Delta\theta_i \\ \Delta V_i \end{bmatrix} \tag{3}$$

where

$$[D']_{(2\times 2)} = [D] - [C]^*[A] - 1^*[B].$$

The (3) expresses the sensitivity relationships between the voltage and the power injections in bus i considering the whole system. From the determinant of D' matrix, it can be concluded that [5]:

1) $\mathbf{det}[\boldsymbol{D'}] > \mathbf{0}$: bus i is operating in the stable region of the PV curve (upper half);
2) $\mathbf{det}[\boldsymbol{D'}] < \mathbf{0}$: bus i is operating in the unstable region of the PV curve (lower half), that is, the bus i has voltage instability problems caused by controllability loss;
3) $\mathbf{det}[\boldsymbol{D'}] = \mathbf{0}$: bus i is operating in the maximum loading point ("tip of the nose").

The D' matrix can be used to obtain an estimate of the VSM for the bus i. It is obtained by the association of a two-bus equivalent system with the D' matrix for the bus i. The derivation of the equivalent system is based on the following characteristics in common between the matrices D' and the Jacobian matrix of a two-bus system: order 2×2 and elements expressing the same sensitivity relationships. Consequently, it is possible to obtain a two-bus equivalent system from the equality between D' matrix and the Jacobian matrix of the equivalent system (J^{eq}). The hypothesis results in the following equation system:

$$\begin{aligned}[J^{eq}] &= [D'] \\ &\Rightarrow \begin{bmatrix} -Q_2^{eq} - \left(V_2^{eq}\right)^2 B_{22}^{eq} & \left(V_2^{eq}\right)^{-1} P_2^{eq} + V_2^{eq} G_{22}^{eq} \\ P_2^{eq} - \left(V_2^{eq}\right)^2 G_{22}^{eq} & \left(V_2^{eq}\right)^{-1} Q_2^{eq} - V_2^{eq} B_{22}^{eq} \end{bmatrix} \\ &= \begin{bmatrix} D'_{11} & D'_{12} \\ D'_{21} & D'_{22} \end{bmatrix} \end{aligned} \tag{4}$$

where:

V_2^{eq}	voltage magnitude in bus 2 of the equivalent system;
D'_{11}, D'_{12}, D'_{21} and D'_{22}	elements of the $D'_{(2\times 2)}$ matrix for bus i;
$G_{22}^{eq}(B_{22}^{eq})$	diagonal element of the nodal conductance susceptibility matrix associated with bus 2 in the equivalent system;
$P_2^{eq}(Q_2^{eq})$	net active (reactive) power injection in bus 2 of the equivalent system.

The equation system (4) has the following characteristics:

1) Four equations: $D'_{11} = J_{11}^{eq}$, $D'_{12} = J_{12}^{eq}$, $D'_{21} = J_{21}^{eq}$, and $D'_{22} = J_{22}^{eq}$;
2) Five unknowns variables: P_2^{eq}, Q_2^{eq}, G_{22}^{eq}, B_{22}^{eq}, and V_2^{eq};
3) Undetermined since the number of equations is lower than the number of unknown variables;
4) Nonlinear because of the product terms such as $\left(V_2^{eq}\right)^2 B_{22}^{eq}$ in the equation $D'_{11} = J_{11}^{eq}$.

Due to the characteristics above it is not possible to obtain the equivalent system parameters using direct methods for the solution of linear systems. This difficult can be overcome considering that the voltage in the bus 2 of the equivalent system is equal to the voltage in the bus i of the multi-node system:

$$V_2^{eq}\angle\theta_2^{eq} = V_i\angle\theta_i. \tag{5}$$

This simplification is acceptable because the voltages in the internal and boundary buses of an equivalent network are equal to their respective values in the original network. In this way, it is possible to simplify the system (4) by the substitution of V_2^{eq} with V_i:

$$\begin{bmatrix} -Q_2^{eq} - V_i^2 B_{22}^{eq} & V_i^{-1} P_2^{eq} + V_i G_{22}^{eq} \\ P_2^{eq} - V_i^2 G_{22}^{eq} & V_i^{-1} Q_2^{eq} - V_i B_{22}^{eq} \end{bmatrix} = \begin{bmatrix} D'_{11} & D'_{12} \\ D'_{21} & D'_{22} \end{bmatrix}. \tag{6}$$

The equation system (6) has four unknowns variables (P_2^{eq}, Q_2^{eq}, G_{22}^{eq}, and B_{22}^{eq}) and four equations ($D'_{11} = J_{11}^{eq}$, $D'_{12} = J_{12}^{eq}$, $D'_{21} = J_{21}^{eq}$, and $D'_{22} = J_{22}^{eq}$). Furthermore, the nonlinear terms were eliminated because V_i is obtained from the power flow solution for the multi-node system. Consequently, it is possible to estimate the equipment system parameters through the linear systems shown in (7) and (8) at the bottom of the page.

The solution of (7) and (8) gives

$$Q_2^{eq} = -\frac{1}{2}\left(D'_{11} - V_i D'_{22}\right)$$
$$B_{22}^{eq} = -\frac{1}{2}\left(\frac{D'_{11}}{V_i^2} + \frac{D'_{22}}{V_i}\right)$$

$$\begin{cases} -Q_2^{eq} - V_i^2 B_{22}^{eq} = D'_{11} \\ V_i^{-1} Q_2^{eq} - V_i B_{22}^{eq} = D'_{22} \end{cases} \Rightarrow \begin{bmatrix} -1 & -V_i^2 \\ V_i^{-1} & -V_i \end{bmatrix} \begin{bmatrix} Q_2^{eq} \\ B_{22}^{eq} \end{bmatrix} = \begin{bmatrix} D'_{11} \\ D'_{22} \end{bmatrix} \tag{7}$$

$$\begin{cases} V_i^{-1} P_2^{eq} + V_i G_{22}^{eq} = D'_{12} \\ P_2^{eq} - V_i^2 G_{22}^{eq} = D'_{21} \end{cases} \Rightarrow \begin{bmatrix} V_i^{-1} & V_i \\ 1 & -V_i^2 \end{bmatrix} \begin{bmatrix} P_2^{eq} \\ G_{22}^{eq} \end{bmatrix} = \begin{bmatrix} D'_{12} \\ D'_{21} \end{bmatrix} \tag{8}$$

$$P_2^{eq} = \frac{1}{2}\left(V_i D'_{12} + D'_{21}\right)$$
$$G_{22}^{eq} = \frac{1}{2}\left(\frac{D'_{12}}{V_i} - \frac{D'_{21}}{V_i^2}\right).$$

At this point, it must be mentioned that the voltage in bus 1 (slack bus) of the equivalent system still had not been determined. The procedure used to estimate the voltage in bus 1 is presented in the Appendix.

The determinant of the matrix J^{eq} can be used to estimate a VSM for bus i since $D' = J^{eq}$. Consequently, det[D'] is given by (9) at the bottom of the page.

Multiplying the right and left sides of (9) by V_i [5] and remembering, from (5), that results in [5]

$$\begin{aligned} V_i \det[D'] &= V_2^{eq} \det[J^{eq}] \\ &= (S_2^{\max})^2 - (S_2^{eq})^2 \\ &= (S_2^{\max} + S_2^{eq})(S_2^{\max} - S_2^{eq}) \end{aligned} \tag{10}$$

where $S_2^{eq} = \sqrt{(P_2^{eq})^2 + (Q_2^{eq})^2}$, $S_2^{\max} = (V_2^{eq})^2 + |Y_{22}^{eq}|$

$$Y_{22}^{eq} = G_{22}^{eq} + jB_{22}^{eq} \quad \text{and}$$
$$|Y_{22}^{eq}| = \sqrt{(G_{22}^{eq})^2 + (B_{22}^{eq})^2}.$$

From (10) it may be concluded that:

1) $\mathbf{det}[\boldsymbol{D'}] > \mathbf{0}$: when $(S_2^{\max} - S_2^{eq}) > 0$ (stable region);
2) $\mathbf{det}[\boldsymbol{D'}] < \mathbf{0}$: when $(S_2^{\max} - S_2^{eq}) < 0$ (unstable region associated with controllability loss);
3) $\boldsymbol{det}[\boldsymbol{D'}] = \mathbf{0}$: when $(S_2^{\max} - S_2^{eq}) = 0$ (maximum loading point).

Consequently, the term $(S_2^{\max} - S_2^{eq})$ can be used to define a VSM to bus $i(M_i)$ as:

1) $\mathbf{det}[\boldsymbol{D'}] > \mathbf{0}$ **(stable region)**: $M_i = 100 \times S_2^{\max} - S_2^{eq}/S_2^{\max}$;
2) $\mathbf{det}[\boldsymbol{D'}] \leq \mathbf{0}$ **(unstable region)**: $M_i = 100 \times S_2^{\max} - S_2^{eq}/S_2^{eq}$.

Using S_2^{eq} as base in the unstable region it avoids the margin M_i going to $-\infty$ as $S_2^{\max} \longrightarrow 0$ in this region [33]. The margin M_i has the following interpretations [5]:

1) **in the stable region**: it is the amount of apparent power that should be added to bus 2 of the equivalent system to achieve the $S_2^{\max}$;
2) **in the unstable region**: it is the amount of apparent power that should be withdrawn from bus 2 of the equivalent system to achieve the $S_2^{\max}$.

It is to be noticed that is not necessary to evaluate the bus 1 voltage to estimate the VSM for the bus i, as (9) and (10) are independent of the bus 1 voltage. However, the existence of a feasible slack bus voltage guarantees the coherence of the equivalent system identification procedure. The procedure to estimate the bus 1 voltage of the equivalent system is presented in the Appendix.

B. Nonlinear OPF

The SRPFE task is performed by the minimization of the power curtailments in the load buses subject to the following constraints: active and reactive power balance equations, limits on the active and reactive power generations and specified ranges for the voltages in a bus with reactive power generation. In this nonlinear OPF problem, the following control actions have been used for the SRPFE: active generation redispatch, voltage resetting in buses with reactive power generation and load curtailment (as a last resource).

The nonlinear OPF problem has been solved using the Interior Point Algorithm proposed in [34]–[36]. The Interior Point Method has the following advantages regarding SLP and SQP:

1) it is not necessary to attain the feasibility of the nonlinear equality constraints (power flow balance equations) at the intermediate iterations of the Interior Point Method as required in the SLP. This characteristic is of vital importance in the SRPFE;
2) the Interior Point Method often (but not always) outperforms active set methods, such as SQP, in large scale applications [37].

Finally, it should be mentioned that the main advantage of using the nonlinear OPF to solve the SRPFE problem is the ability of this approach to identify whether it is necessary to carry out load curtailments to eliminate the unsolvability. The identification is not possible when the solution of the SRPFE is based on the Continuation Power Flow method [7], because the load and the generation are simultaneously reduced or increased in each predictor/corrector step.

System states with heavy load conditions or high levels of reactive power may result in convergence problems for the OPF algorithm used in the RESFLUP. These nonconvergence problems of the OPF algorithm are overcome using the following strategies:

1) Restart of the OPF algorithm with a safeguard parameter set for the Interior-Point Method. For example, the step length of the Interior-Point Method is reduced when there is a convergence failure of the RESFLUP algorithm.
2) Enlargement of the voltage ranges for PV and Vθ buses. This strategy is very efficient to eliminate infeasibility problems caused by high levels of reactive power. In these

$$\det[D'] = \det[J^{eq}]$$
$$\det[D'] = (V_2^{eq})^3 \left((G_{22}^{eq})^2 + (B_{22}^{eq})^2\right) - (V_2^{eq})^{-1} \left((P_2^{eq})^2 + (Q_2^{eq})^2\right) \tag{9}$$

cases, the terminal voltages in reactive generation buses tend to increase.

Finally, it is important to mention that there are system states in which the OPF convergence problems are untreatable. These states are banned of the system states sample used to estimate the probabilistic indices.

IV. Proposed Indices for VSPA

The proposed method for VSPA (see Section II) has been used to evaluate the following indices: VIR, expected nodal VSM, and Well-Being states probabilities. The Well-Being analysis has the objective of establishing a link between probabilistic analysis and power system operation, which traditionally has been dominated by deterministic criteria such as the N-1. This link is based on the definition of Well-Being states, which are similar to the states used in the power system security assessment [38]. Therefore, system operators who are used to the deterministic approaches may easily interpret Well-Being indices, which embed probabilistic information in accepted deterministic criteria [19]–[21]. In this paper, the deterministic criterion used to define Well-Being states is the occurrence of voltage instability problems. This criterion was chosen because it has been used by the Brazilian independent system operator in voltage security studies [39]. With the established criterion, it is possible to define the following Well-Being states:

1) **Health state**: the power equations have a solution and $M^j_{\min} > 0$, where $M^j_{\min} = \min\left\{M^j_i, i \in (\Omega_{PQ} \cup \Omega_{PV})\right\}$, M^j_i is the VSM for bus i in the state j, $M^j_{\min}$ is the minimum VSM for all the buses in the state j and $\Omega_{PQ}(\Omega_{PV})$ is the set of PQ (PV) buses;
2) **Marginal state**: the power flow equations have a solution and $M^j_{\min} \leq 0$;
3) **Emergency state**: the power flow equations have no solution. However, the solvability restoration may be obtained without load curtailment;
4) **Collapse state**: the power flow equations have no solution and load curtailment is necessary for the solvability restoration.

The probabilistic indices cited above have the following test functions:

1) **VIR**

$$F\left(s^j\right) = \begin{cases} 1, & \text{if } s^j \in \Omega_\phi \text{ or } M^j_{\min} \leq 0 \\ 0, & \text{otherwise} \end{cases}$$

where $\Omega\phi$ is the set of unsolvable states.

2) **Nodal expected VSM**

$$F\left(s^j\right) = M^j_i \text{ if } s^j \notin \Omega_\phi \text{ and } i \in (\Omega_{PQ} \cup \Omega_{PV}).$$

3) **P(Health)**

$$F\left(s^j\right) = \begin{cases} 1, & \text{if } s^j \notin \Omega_\phi \text{ and } M^j_{\min} > 0 \\ 0, & \text{otherwise.} \end{cases}$$

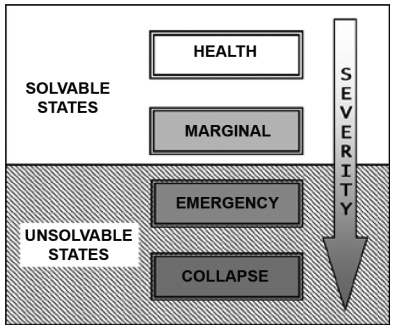

Fig. 2. Well-Being states used in VSPA.

4) **P(Marginal)**

$$F\left(s^j\right) = \begin{cases} 1, & \text{if } s^j \in \Omega_\phi \text{ and } R^j_{TOT} < \varepsilon_{LC} \\ 0, & \text{otherwise.} \end{cases}$$

5) **P(Emergency)**

$$F\left(s^j\right) = \begin{cases} 1, & \text{if } s^j \in \Omega_\phi \text{ and } R^j_{TOT} \geq \varepsilon_{LC} \\ 0, & \text{otherwise} \end{cases}$$

where ε_{LC} is the load curtailment tolerance $\varepsilon_{LC} = 0.01$ MW and R^j_{TOT} is the total load curtailment required for SRPFE in the state s^j.

6) **P(Collapse)**

$$F(s^j) = \begin{cases} 1, & \text{if } s^j \in \Omega_\phi \text{ and } avR^j_{TOT} \geq \epsilon_{LC} \\ 0, & \text{otherwise.} \end{cases}$$

From the test functions defined above, it may be concluded that:

1) The voltage instability problems caused by unsolvability can be considered more severe than those associated with controllability loss. This assumption is also used in the contingency ranking for voltage stability assessment [40];
2) The Well-Being states are defined in accordance with the severity of the voltage instability mechanisms, that is: controllability loss and unsolvability. The Well-Being states in ascending order of severity are shown in Fig. 2;
3) The nodal VSM is evaluated only for solvable states. The constraint is due to the operation point, obtained by the SRPFE algorithm (nonlinear OPF), being associated with a new load/generation pattern. Consequently, the VSM evaluated after the SRPFE has no association with the distance between the solvability boundary and the original infeasible operation point. Furthermore, it should be remembered that unsolvable states are considered more critical than those with controllability loss. Due to this, there is no sense in evaluating the expected nodal VSM for states with unsolvability problems.

V. Test Results

The results obtained with the proposed method for the VSPA are presented in this section. The models and techniques described in the previous sections have been applied to three test

TABLE I
CHARACTERISTICS OF THE TEST SYSTEMS

Characteristic	Systems		
	MRTS	BTS-65	BTS-107
Installed Capacity (MW)	4304.0	17858.2	22080.2
Load Peak (MW)	3562.4	10102.1	12681.7
No. of buses	24	65	107
No. of circuits	31	141	230
No. of generators	40	65	103
No. of plants	10	14	23
No. of compensators	1	4	5

systems. The following indices have been estimated: VIR, probabilities of Well-Being states and expected values of the nodal VSM. The results presented in the following subsections are organized as:

1) Section V-A contains a general description of the test systems;
2) the accuracy and the computational costs of the proposed method for the VSPA are discussed in Section V-B;
3) the VSPA based on the system indices: VIR, probabilities of the Well-Being states and participation factors in the VIR are presented in Section V-C;
4) in Section V-D it is shown that the expected values of the nodal VSM can be used to identify critical bus and areas in the VSPA.

A. Characteristics of the Test Systems

The proposed method for the VSPA has been tested in three test systems: two equivalent systems obtained from the Brazilian interconnected power system [22] (STB-65 and STB-107) and a modified version of the IEEE system of 24 buses [23], [24] (MRTS). The main characteristics of these test systems are presented in Table I. The reliability data associated with the systems BTS-65 and BTS-107 have been obtained from [41].

The BTS-65 is composed of the South and South-East areas of the interconnected Brazilian power system, while the BTS-107 is composed of the areas of: Mato Grosso, the South, and South-East. In these systems the generation is predominantly hydroelectric, while in the MRTS generation is predominantly thermal.

The MRTS has been used due to its transmission networks being heavily loaded. The Brazilian systems are used because their generation plants are located far from the load centers. Therefore, there are long transmission trunks transporting large energy blocks in the two Brazilian systems. Consequently, the three test systems are suitable for voltage instability studies.

B. Assessment of the Accuracy and Computational Effort

The probabilistic indices used in VSPA have been estimated under the following conditions:

1) the load forecasting error (σ^0) is 5.0%;
2) outages in circuits, generators, and compensators have been considered in the VSPA;

TABLE II
COMPUTATIONAL EFFORT TO CARRY OUT THE VSPA IN THE TEST SYSTEMS

System	No. of Simulations	Computational Time (min.)
MRTS	42,401	4.5036
BTS-65	38529	7.3208
BTS-107	30313	15.9107

3) the pre-specified tolerances for the coefficient of variation in the systems BTS-65, BTS-107 and MRTS are equal to: 5.0%, 10.0% and 5%, respectively;
4) $\mathrm{NS}^{\max}$ is 100 000 for the MRTS and 50 000 for the Brazilian systems;
5) the VSPA is carried out considering a two state model for generation failures. This simplification is due to a lack of data associated with multi-state models in the Brazilian systems;
6) the relative weights for each power plant of the Brazilian systems are based on the equivalent reactance from the bus in which the plant is connected. This procedure is applied because several Brazilian electric energy utilities use the inverse of the equivalent reactances as participation factors in the hydroelectric dispatch.

The computational effort (number of simulations and CPU time) to carry out VSPA in each test system, considering the conditions 1)-4), is shown in Table II. The results presented in this table have been obtained using a PC with Intel Core Quad CPU of 2.4 GHz and 3.25 GB of RAM.

From the Table II, it can be concluded that the sample size required estimating a probabilistic index, with a specified precision, is independent of the system size (number of components). For example, the sample size for the MRTS (42 401) is bigger than the one associated with the BTS-65 (38 529), for a relative uncertainty of 5%. Nevertheless, the MRTS is about three times as small as the BTS-65. This effect is due to the number of simulations being evaluated by

$$NS = \frac{\tilde{V}ar(F)}{[\beta^{spe}\tilde{E}(F)]^2}$$

where β^{spe} is the specified value for the coefficient of variation. Consequently, indices with large variances and/or small expected values demand a huge number of simulations to satisfy a specified tolerance. The small expected value of an index can be associated with a rare event probability. For example, the expected value of the marginal state probability in the BTS-107 is equal to 3.2889×10^{-3}. Consequently, the sample size required to estimate this probability for a relative uncertainty of 5% is

$$NS = \frac{1 - \mathrm{P(marginal)}}{(\beta^{spe})^2\,\mathrm{P(marginal)}} = \frac{1 - 3.2889 \times 10^{-3}}{(0.05)^2\, 3.2889 \times 10^{-3}} \approx 120\,856.$$

The assessment of a system states sample with 120 856 elements causes a significant increase in the computation time of

TABLE III
COEFFICIENT OF VARIATION FOR THE PROBABILISTIC INDICES (IN PERCENTAGE)

Index	MRTS	BTS-65	BTS-107
VIR	0.8120	1.1401	1.2774
P(Health)	0.2905	0.2277	0.2583
P(Marginal)	4.9954	1.2431	9.9837
P(Emergency)	0.8624	4.5552	1.3566
P(Collapse)	4.1752	4.9994	5.0311
Expected Nodal VSM	0.6992	0.6068	0.1712

TABLE IV
ROOT CAUSE ANALYSIS OF THE VIR BASED ON THE SYSTEM UNCERTAINTIES

Uncertainties	MRTS	BTS-65	BTS-107
G	69.8980 %	17.6049%	57.4147%
C	0.9846 %	29.0816%	6.6104%
GC	4.2338 %	11.8821%	31.6987%
L	24.8836 %	41.4315%	4.2762%

the APET for large scale systems. Due to this, a relative uncertainty of 10% has been used for the MCSM in the BTS-107. This procedure did not reduce the accuracy of any indices estimated for the BTS-107 because their expected values are bigger than P(marginal). The estimated values of β for the probabilistic indices evaluated for the three test systems are shown in Table III. In this table, the β associated with the expected value of the nodal VSM is equal to the maximum β of the VSM for all system buses.

From Table III, it can be concluded that the convergence of the MCSM is dominated by the probabilities of the Well-Being states. For example, the maximum relative uncertainties for the systems MRTS, BTS-65, and BTS-107 are associated with the following indices: P(Marginal), P(Collapse), and P(Marginal), respectively. This characteristic is due to probabilities of these states have the smallest expected values among the estimated indices.

C. VIR and Probabilities of the Well-Being States

The VIR for the systems MRTS, BTS-65, and BTS-107 are, respectively, 26.3484%, 16.6446% ,and 16.8179%. These results demonstrate that the VIR for the three test systems is very large. However, the causes of the high risk values are not the same for the three test systems. This fact can be demonstrated through the evaluation of the participation factors of the uncertainties in the VIR. That is, the percentage of each type of uncertainty in the VIR. These participation factors allow carrying out a root cause analysis of the VIR oriented for the system uncertainties. The participation factors of the uncertainties in the VIR are presented in Table IV.

From Table IV, it can be concluded that:

1) the unstable states of the MRTS and BTS-107 systems are mainly caused by generator failures. This effect may be caused by the existence of a deficiency in the reactive power generation reserve. Consequently, there are not enough Mvar resources to correct the voltage profile in the contingency states;

TABLE V
PROBABILITIES OF THE WELL-BEING STATES

Sates	MRTS	BTS-65	BTS-107
Health	7.3652×10^{-1}	8.3355×10^{-1}	8.3182×10^{-1}
Marginal	9.3630×10^{-3}	1.4381×10^{-1}	3.2989×10^{-3}
Emergency	2.4077×10^{-1}	1.2354×10^{-2}	1.5201×10^{-1}
Collapse	1.3349×10^{-2}	1.0278×10^{-2}	1.2866×10^{-2}

TABLE VI
PARTICIPATION FACTORS OF THE UNSTABLE WELL-BEING STATES ON THE VIR

States	MRTS	BTS-65	BTS-107
Marginal	3.5535 %	86.4026%	1.9616%
Emergency	91.3802 %	7.4224%	90.3884%
Collapse	5.0662 %	6.1750%	7.6501%

2) in BTS-65, the main cause of the voltage instability problems is the load forecasting error. This result is an indicative that the current operating point in the BTS-65 corresponds to a heavily load condition. Consequently, small fluctuations in the system peak load result in voltage instability scenarios;
3) the system where the transmission failures have more impact on the VIR is the BTS-65. Thus, it may be necessary reinforcements in the transmission network.

The VSPA of the test systems has also been carried out using Well-Being indices. They allow a voltage stability analysis based on the instability mechanisms. Furthermore, the Well-Being analysis also enables the identification of unsolvable states which can be restored without using load curtailment. The probabilities of the Well-Being states for the three test systems are presented in Table V. They can be used to estimate the participation factors of the unstable Well-Being states (Marginal, Emergency, and Collapse) on the VIR. That is, it is possible to use the probabilities of the unstable Well-Being states to carry out a root cause analysis of the VIR oriented for the voltage instability mechanisms. The participation factors of the Marginal, Emergency, and Collapse states are shown in Table VI.

From Tables V and VI, it can be stated that:

1) the emergency state is the most likely state in the MRTS and BTS-107 systems. In other words, in these systems the main cause of the voltage instability is the unsolvability. This fact is also demonstrated by the participation factors. The participation factors of the emergency state for the systems MRTS and BTS-107 are equal to 91.3802% and 90.3884%, respectively. That is, the largest participation factors of the emergency are associated with the systems MRTS and BTS-107;
2) the maximum value of the probability of occurrence of the marginal state is associated with the BTS-65 system. Due to this, the largest participation factor of the marginal state occurs in the BTS-65 system (86.4026%). That is, in the BTS-65 the unstable states are mainly caused by the controllability loss;
3) the participation factors associated with the collapse state are small for the three systems. For example, the maximum

TABLE VII
EFFICIENCY OF THE CONTROL ACTIONS USED IN THE SRPFE

State	MRTS	BTS-65	BTS-107
Emergency	94.7471 %	54.5872%	92.1969%
Collapse	5.2529 %	45.4128%	7.8031%

value of the participation factor, associated with the collapse state, for the test systems is equal to 7.6501%. Consequently, even in the most unsolvable states it is possible to restore a solution without using load curtailment. Therefore, the unsolvability of the power flow equations for the three systems is not too severe.

Additionally, it is also important to assess the efficiency of the control actions used for the SRPFE. This assessment may be carried out by the evaluation of the participation factors of the unsolvable Well-Being States (Emergency and Collapse) with reference to the probability of unsolvability. These participation factors are presented in Table VII for the three test systems.

In Table VII, it can be observed that the generation redispatch and the voltage set-point resetting in PV and $V\theta$ buses are highly efficient in eliminating the unsolvability problems in the MRTS and BTS-107 systems. For example, the minimum value of the participation factor associated with the emergency state in these systems is equal to 92.1969%. That is, the maximum percentage of unsolvable states which require load curtailments in the SRPFE is 7.8031%. On the other hand, the corrective actions used in the SRPFE are efficient in 54.5872% in the BTS-65 system. Consequently, the unsolvability of the power flow equations is more severe in this system.

Finally, it should be mentioned that there are system states undergoing controllability loss after the SRPFE. This result is due to the lack of voltage stability constraints in the OPF algorithm used to carry out the SRPFE. Consequently, a restored solution by the OPF algorithm may have controllability loss problems. That is, the solution obtained by the SRPFE algorithm is in the unstable region (lower half) of the PV curve. The probabilities of a state having unsolvability and voltage controllability loss problems for the MRTS, BTS-65, and BTS-107 systems are, respectively, 0.0684%, 2.0945%, and 4.9682%. From these results, it can be noted that the probability of occurrence of the two voltage instability mechanisms is significant in the Brazilian systems. For example, the minimum value of this probability in the BTS-65 and BTS-107 systems is 2.0945%.

D. Identification of Critical Buses and Areas Using the Expected Nodal VSM

In this section, the expected values of the nodal VSM are used to identify critical buses and areas in the BTS-107 system. This identification is based on the Influence Index [40]. This index is given by $II_i^j = 100\% \times \left(M_i^j/M_i^0 - 1\right)$, where M_i^j (M_i^0) is the VSM of the bus i for the contingency state j (base case condition), II_i^j is the Influence Index of the bus i for the contingency state j.

Consequently, the expected value of the Influence Index is given by $\tilde{E}(II_i) = 100\% \times \left(\tilde{E}(M_i)/M_i^0 - 1\right)$. It indicates the percentage of the VSM associated with the base case, which is modified in the presence of the system uncertainties. Usually, this index is negative, meaning that the VSM of the base case is reduced in the presence of system uncertainties. Consequently, the buses with the smallest Influence Index are more vulnerable to voltage instability problems. The expected values of the Influence Index for 21 buses of each area of the BTS-107 system are shown in Table VIII. From this table, it can be concluded that the smallest values of the Influence Index are associated with the areas Mato Grosso and South-East. From this table, it can be noted that the values of the Influence Index concerning to the South area are less negative than those associated with the South-East and Mato Grosso areas. For example, the minimum values of the Influence Index for the South, South-East, and Mato Grosso areas are equal to -1.4219%, -4.6323%, and -7.3864%, respectively. In other words, the South area is more stable than the South-East and Mato Grosso areas. On the other hand, it can be noted that the Mato Grosso area is the most vulnerable area to voltage instability problems in the BTS-107 system. It is due to the topology of the Mato Grosso area being basically radial. Consequently, there are few paths to power transfers for the load buses. Therefore, the loading margin of the Mato Grosso area is lower than the margins of the other areas.

TABLE VIII
EXPECTED INFLUENCE INDEX FOR THE BTS-107

South Area		South-East Area		Mato Grosso Area	
Bus Number	$\tilde{E}(II_i)$	Bus Number	$\tilde{E}(II_i)$	Bus Number	$\tilde{E}(II_i)$
960	-1.4219	231	-4.6323	4596	-7.3864
959	-1.4058	48	-2.2917	4703	-6.4573
895	-1.3888	104	-1.6115	4533	-6.4462
939	-1.3385	106	-1.5317	4532	-6.3787
814	-1.2939	1503	-1.4915	4542	-6.3340
938	-1.2887	140	-1.4889	4522	-6.3281
1015	-1.0766	225	-1.2625	4623	-6.1850
834	-1.0330	1504	-0.8543	4530	-6.1818
1047	-0.5758	123	-0.8438	4862	-6.1068
898	-0.5733	103	-0.8067	4592	-6.0294
839	-0.4973	122	-0.7916	4521	-5.9034
1210	-0.4519	102	-0.6627	4807	-5.8439
2458	-0.4181	138	-0.6354	4501	-5.8259
848	-0.3704	126	-0.6018	4523	-5.7417
933	-0.3490	86	-0.4707	4805	-5.6479
934	-0.3396	233	-0.4678	4552	-5.4928
840	-0.3292	218	-0.4498	4804	-5.1126
824	-0.3236	234	-0.4296	21	-4.6173
976	-0.2477	219	-0.4296	4572	-4.5805
896	-0.1756	16	-0.4226	4562	-3.9917
965	-0.1598	210	-0.4025	4582	-3.4187

Additionally, in Table VIII it is also shown that the buses of the South-East area underwent significant reductions in the VSM. For example, the biggest reduction in the nodal VSM for the South-East area is equal to -4.6323% in bus 231.

VI. CONCLUSIONS

This paper has described a method of including unsolvability and voltage controllability loss in the VSPA. This method is based on the combination of three techniques: DMM, nonlinear

OPF and MCSM. The results obtained with the proposed approach in the test systems demonstrate that:

1) load forecasting errors may have a significant participation factor on the VIR;
2) unstable states associated with controllability loss have considerable probability of occurrence;
3) the expected values of the nodal VSM can be used to identify vulnerable buses and areas to voltage instability problems;
4) the SRPFE may result in states with controllability loss;
5) the control actions used in the SRPFE have proved to be very efficient in most of the test systems.

APPENDIX

The estimation of the voltage in bus 1 of the equivalent system should ensure the solvability of the power flow equations, that is

$$\begin{aligned} P_2^{eq} - \left(V_2^{eq}\right)^2 G_{22}^{eq} = & - V_2^{eq} V_1^{eq} g_{21}^{eq} \cos\left(\theta_2^{eq} - \theta_1^{eq}\right) \\ & - V_2^{eq} V_1^{eq} b_{21}^{eq} \sin\left(\theta_2^{eq} - \theta_1^{eq}\right) \quad (11) \\ Q_2^{eq} + \left(V_2^{eq}\right)^2 B_{22}^{eq} = & - V_2^{eq} V_1^{eq} g_{21}^{eq} \sin\left(\theta_2^{eq} - \theta_1^{eq}\right) \\ & + V_2^{eq} V_1^{eq} b_{21}^{eq} \cos\left(\theta_2^{eq} - \theta_1^{eq}\right) \quad (12) \end{aligned}$$

where g_{21}^{eq} (b_{21}^{eq}) is the conductance susceptibility of the series branch between the buses 1 and 2 of the equivalent system.

Equations (11) and (12) can be simplified using the expressions

$$J_{21}^{eq} = P_2^{eq} - \left(V_2^{eq}\right)^2 G_{22}^{eq} \quad (13)$$

$$-J_{11}^{eq} = Q_2^{eq} + \left(V_2^{eq}\right)^2 B_{22}^{eq}. \quad (14)$$

Replacing (13) and (14) in (11) and (12), respectively, results in

$$\begin{aligned} J_{21}^{eq} = & - V_2^{eq} V_1^{eq} g_{21}^{eq} \cos\left(\theta_2^{eq} - \theta_1^{eq}\right) \\ & - V_2^{eq} V_1^{eq} b_{21}^{eq} \sin\left(\theta_2^{eq} - \theta_1^{eq}\right) \quad (15) \\ -J_{11}^{eq} = & - V_2^{eq} V_1^{eq} g_{21}^{eq} \sin\left(\theta_2^{eq} - \theta_1^{eq}\right) \\ & + V_2^{eq} V_1^{eq} b_{21}^{eq} \cos\left(\theta_2^{eq} - \theta_1^{eq}\right). \quad (16) \end{aligned}$$

Additionally, the derivation hypothesis of the equivalent system establishes that $V_2^{eq}\angle\theta_2^{eq} = V_i\angle\theta_i$ and $J^{eq} = D'$. In this way, it is possible to rewrite (15) and (16) as

$$F_1(z) = 0 \quad (17)$$

$$F_2(z) = 0 \quad (18)$$

where

$$\begin{aligned} F_1(z) = & D'_{21} + V_i V_1^{eq} g_{21}^{eq} \cos\left(\theta_i - \theta_1^{eq}\right) \\ & + V_i V_1^{eq} b_{21}^{eq} \sin\left(\theta_i - \theta_1^{eq}\right) \\ F_2(z) = & D'_{11} + V_i V_1^{eq} g_{21}^{eq} \sin\left(\theta_i - \theta_1^{eq}\right) \\ & - V_i V_1^{eq} b_{21}^{eq} \cos\left(\theta_i - \theta_1^{eq}\right) \\ z = & \left[\theta_1^{eq} \quad V_1^{eq} \quad g_{21}^{eq} \quad b_{21}^{eq}\right]. \end{aligned}$$

The equation system (17) and (18) is nonlinear and underdetermined. In other words, the number of equations (two) is lower than the number of variables (four). Nevertheless, it is possible to solve a nonlinear underdetermined system using the Newton–Raphson algorithm. The approach has been used in [42] to correct the voltage profile of an electric network. However, the Taylor series expansion of the equations results in the linear undetermined system:

$$\nabla_z F(z^k)\Delta z^k = -F\left(z^k\right) \quad (19)$$

where

$\nabla_z F(z^k) = \left[\nabla_z F_1(z^k) \quad \nabla_z F_2(z^k)\right]^T$ is the Jacobian matrix (with dimension 2×4) in (17) and (18).

$F\left(z^k\right) = \left[F_1(z^k) \quad F_2(z^k)\right]^T$ is the mismatch vector (with dimension 2×1) for (17) and (18).

$z^k(\Delta z^k)$ is the estimate (correction) of the vector z for the iteration k of the Newton-Raphson algorithm.

The solution of the linear system (19) is associated with the optimization problem:

$$\text{Min} \quad \left(\Delta z^k\right)^T \Delta z^k \quad (20)$$

$$\text{Subject to:} \quad \nabla_z F(z^k)\Delta z^k = -F\left(z^k\right). \quad (21)$$

An optimization problem with the formulation analogous to (20) and (21) is denominated as the Linear Minimum-Norm Problem [43]. The solution of this problem is given by

$$\Delta z^k = -A^+ F\left(z^k\right) \quad (22)$$

where $A^+ = \nabla_z F\left(z^k\right)^T \left[\nabla_z F\left(z^k\right) \nabla_z F\left(z^k\right)^T\right]^{-1}$ is the pseudo-inverse matrix of $\nabla_z F\left(z^k\right)$ [43].

In this way, in each iteration of the Newton–Raphson algorithm the corrections of the equivalent system parameters are estimated by (22). It should be mentioned that the Δz^k evaluation has low computational cost because the matrices used in this computation have small dimensions. Therefore, it is possible to obtain an analytical expression for the vector Δz^k.

As well as the power flow based on the Newton–Raphson algorithm, the parameter estimation algorithm of the equivalent system will have convergence problems in the presence of a poor starting point. In this paper vector z^0 is defined based on the following equations:

$$g_{21}^{eq} = \frac{1}{V_i V_1^{eq}} \left[-\sin\theta_{i1} D'_{11} + \cos\theta_{i1} D'_{21}\right] \quad (23)$$

$$b_{21}^{eq} = \frac{1}{V_i V_1^{eq}} \left[\cos\theta_{i1} D'_{11} + \sin\theta_{i1} D'_{21}\right] \quad (24)$$

where $\theta_{i1} = \theta_i - \theta_1$

Equations (23) and (24) have been obtained from the equalities: $V_2^{eq}\angle\theta_2^{eq} = V_i\angle\theta_i$ and $[D'] = [J^{eq}]$(with the J^{eq} elements expressed by trigonometric functions). They may be linearized using the following approximations: $V_1^{eq} \approx 1.0$, $V_i \approx 1.0$,

$\sin\theta_{i1} \approx \theta_{i1}$, and $\cos\theta_{i1} \approx 1.0$. Introducing the approximations into (23) and (24) results in

$$\begin{bmatrix} 1 & 0 & -D'_{11} \\ 0 & 1 & -D'_{21} \end{bmatrix} \begin{bmatrix} g_{21}^{eq} \\ b_{21}^{eq} \\ \theta_{i1} \end{bmatrix} = \begin{bmatrix} -D'_{21} \\ -D'_{11} \end{bmatrix}. \tag{25}$$

Consequently, the initial values of g_{21}^{eq}, b_{21}^{eq} and θ_1^{eq} ($\theta_1^{eq} = \theta_{i1} - \theta_i$) can also be estimated using the solution of a linear Minimum-Norm Problem.

The authors tested the described algorithm in this appendix in all sampled states of the three test systems. The results obtained with these tests have shown that the proposed algorithm does not have any convergence problems in the solution of the system (17) and (18).

ACKNOWLEDGMENT

The authors would like to thank Dr. M. T. Schilling (UFF-Brazil) and Mr. W. Fernandes Alves (EletroBrás-Brazil) for the availability of data associated with BTS-65 and BTS-107 test systems and for the information concerning the participation factors used in hydroelectric generation dispatch.

REFERENCES

[1] P. Kundur, *Power System Stability and Control*. New York: McGraw-Hill, 1994.
[2] V. Ajjarapu, *Computational Techniques for Voltage Stability Assessment and Control*. New York: Springer, 2006.
[3] T. J. Overbye, "A power flow measure for unsolvable cases," *IEEE Trans. Power Syst.*, vol. 9, no. 3, pp. 1359–1365, Aug. 1994.
[4] S. Granville, J. C. O. Mello, and A. C. G. Melo, "Application of interior point methods to power flow unsolvability," *IEEE Trans. Power Syst.*, vol. 11, no. 2, pp. 1096–1103, May 1996.
[5] R. B. Prada, E. G. C. Palomino, J. O. R. dos Santos, and L. A. S. Pilloto, "Voltage stability assessment for real-time operation," *Proc. Inst. Elect. Eng., Gen., Transm., Distrib.*, vol. 149, no. 2, pp. 175–181, Mar. 2002.
[6] B. Gao, G. K. Morison, and P. Kundur, "Voltage stability evaluation using modal analysis," *IEEE Trans. Power Syst.*, vol. 7, no. 4, pp. 1529–1542, Nov. 1992.
[7] V. Ajjarapu and C. Christy, "The continuation power flow: A tool for steady state voltage stability analysis," *IEEE Trans. Power Syst.*, vol. 7, no. 1, pp. 416–422, Feb. 1992.
[8] R. Billinton and R. N. Allan, *Reliability Evaluation of Power Systems*, 2nd ed. New York: Plenum, 1996.
[9] R. Billinton and W. Li, *Reliability Assessment of Electric Power Systems Using Monte Carlo Methods*. New York: Plenum, 1994.
[10] A. C. G. Melo, J. C. O. Mello, and S. Granville, "The effect of voltage collapse problems in the reliability evaluation of composite systems," *IEEE Trans. Power Syst.*, vol. 12, no. 1, pp. 480–488, Feb. 1997.
[11] R. Billinton and S. Aboreshaid, "Voltage stability considerations in composite power system reliability evaluation," *IEEE Trans. Power Syst.*, vol. 13, no. 2, pp. 655–660, May 1998.
[12] W. Li, Y. Mansour, E. Vaahedi, and D. N. Pettet, "Incorporatiing of voltage stability operation limits in composite systems adequacy assessment: BC hydro's experience," *IEEE Trans. Power Syst.*, vol. 13, no. 4, pp. 1279–1284, Nov. 1998.
[13] S. Aboreshaid and R. Billinton, "Probabilistic evaluation of voltage stability," *IEEE Trans. Power Syst.*, vol. 14, no. 1, pp. 342–348, Feb. 1999.
[14] A. M. Leite da Silva, I. P. Coutinho, A. C. Zambroni de Souza, R. B. Prada, and A. M. Rei, "Voltage collapse risk assessment," *Elect. Power Syst. Res.*, vol. 54, pp. 221–227, Jun. 2000.
[15] H. Wan, J. D. McCalley, and V. Vittal, "Risk based voltage security assessment," *IEEE Trans. Power Syst.*, vol. 15, no. 4, pp. 1247–1254, Nov. 2000.
[16] G. M. Huang and N. C. Nair, "Voltage stability constrained load curtailment procedure to evaluate power system reliability measures," in *Proc. 2002 IEEE Power Eng. Soc. Winter Meeting*, pp. 761–765.
[17] P. Kessel and H. Glavitsch, "Estimating the voltage stability of a power system," *IEEE Trans. Power Del.*, vol. 1, no. 3, pp. 346–354, Jul. 1986.
[18] A. C. Zambroni de Souza, "Tangent vector applied to voltage collapse and loss sensitivity studies," *Elect. Power Syst. Res.*, vol. 47, pp. 65–70, Oct. 1998.
[19] R. Billinton and R. Karki, "Capacity reserve assessment using system well-being analysis," *IEEE Trans. Power Syst.*, vol. 14, no. 2, pp. 433–438, May 1999.
[20] M. Fotuhi-Firuzabad and R. Billinton, "A energy base approach to evaluate interruptible load carryng capability in isolated and interconnected systems including well-being constraints," *IEEE Trans. Power Syst.*, vol. 12, no. 2, pp. 1676–1681, May 1997.
[21] A. M. Leite da Silva, L. C. Resende, L. A. F. Manso, and R. B. Billinton, "Well-Being analysis for composite generation and transmission systems," *IEEE Trans. Power Syst.*, vol. 19, no. 4, pp. 1763–1770, Nov. 2004.
[22] W. F. Alves, "Proposition of test systems to power systems analysis," M.Sc. thesis, Inst. Comput. Fluminense Federal Univ. (UFF), Niterói, RJ, Brazil, 2007, in Portuguese.
[23] O. Bertoldi, L. Salvaderi, and S. Scalcino, "Monte Carlo approach in planning studies—An application to IEEE RTS," *IEEE Trans. Power Syst.*, vol. 3, no. 3, pp. 1146–1154, Aug. 1988.
[24] "IEEE committee report, IEEE reliability test system," *IEEE Trans. Power App. Syst.*, vol. PAS-98, pp. 2047–2054, Nov./Dec. 1979.
[25] R. Billinton and D. Huang, "Effects of load forecast uncertainty on bulk electric system reliability evaluation," *IEEE Trans. Power Syst.*, vol. 23, no. 2, pp. 418–424, May 2008.
[26] B. R. Preiss, *Data Structures and Algorithms with Object-Oriented Design Patterns in* C++. New York: Wiley, 1999.
[27] A. R. L. Oliveira, S. Soares, and L. Nepomuceno, "Short term hydroelectric scheduling combining network flow and interior point approaches," *Int. J. Elect. Power Energy Syst.*, vol. 27, pp. 91–99, Feb. 2005.
[28] J. C. O. Mello, A. C. G. Mello, S. P. Roméro, G. C. Oliveira, S. H. F. Cunha, M. M. Filho, and R. N. F. Filho, "Development of a composite system reliability program for large hydrothermal power systems—Issues and solutions," in *Proc. 3rd Int. Conf. Probabilistic Methods Applied to Electric Power Systems (3rd PMAPS)*, London, U.K., 1991, pp. 64–69.
[29] A. C. G. Melo, J. C. O. Mello, G. C. Oliveira, S. P. Roméro, and R. N. F. Filho, "Probabilistic adequacy evaluation of large scale power systems—A Brazilian case," in *Proc. Stockholm Power Tech Conf.*, Stockholm, Sweden, 1995, pp. 132–137.
[30] M. Montagna and G. P. Granelli, "Detection of Jacobian singularity and network islanding in power flow computations," *Proc. Inst. Elect. Eng., Gen., Transm., Distrib.*, vol. 142, no. 6, pp. 589–594, Nov. 1995.
[31] A. J. Wood and B. F. Wollenberg, *Power Generation, Operation and Control*, 2nd ed. New York: Wiley, 1996.
[32] M. V. F. Pereira and N. J. Balu, "Composite generation/transmission reliability evaluation," *Proc. IEEE*, vol. 80, no. 4, pp. 470–491, Apr. 1992.
[33] R. F. França, "Indices and margins for voltage security assessment," M.Sc. thesis, Elect. Eng. Dept., Catholic Univ. Rio de Janeiro (PUC-Rio), Rio de Janeiro, RJ, Brazil, 2003, in Portuguese.
[34] S. Granville, "Optimal reactive dispatch through interior point methods," *IEEE Trans. Power Syst.*, vol. 9, no. 1, pp. 136–146, Feb. 1994.
[35] R. J. Vanderbei and D. F. Shanno, "An interior point algorithm for nonconvex nonlinear programming," *Comput. Optim. Appl.*, vol. 13, pp. 231–252, Apr. 1999.
[36] A. Wächter and L. T. Biegler, "On the implementation of an interior-point filter line-search algorithm for large scale nonlinear programming," *Math. Program.*, vol. 106, pp. 25–57, May 2006.
[37] J. Nocedal and S. J. Wright, *Numerical Optimization*, 2nd ed. New York: Springer, 2006.
[38] "Task force 38.03.12, power system security assessment: A position paper," *Electra*, no. 175, pp. 49–77, Dec. 1997.
[39] Operador Nacional do Sistema Elétrico, Procedimentos de Rede, Submódulo 23.3, Diretrizes e Critérios para Estudos Elétricos, 2007, in Portuguese. [Online]. Available: http://www.ons.org.br.
[40] R. D. de Moura and R. B. Prada, "Contingency screening and ranking method for voltage stability assessment," *Proc. Inst. Elect. Eng., Gen., Transm., Distrib.*, vol. 152, no. 6, pp. 891–898, Nov. 2005.
[41] M. T. Schilling, J. C. Stacchini de Souza, and M. B. do Couto Filho, "Power system probabilistic reliability assessment: Current procedures in Brazil," *IEEE Trans. Power Syst.*, vol. 23, no. 3, pp. 868–876, Aug. 2008.

[42] R. Travassos, "Voltage profile correction through a power flow algorithm with reactive implicit coupling," M.Sc. thesis, Elect. Eng. Dept., Catholic Univ. Rio de Janeiro (PUC-Rio), Rio de Janeiro, RJ, Brazil, 1992, in Portuguese.
[43] A. Monticelli, *State Estimation in Electric Power Systems: A Generalized Approach*. Norwell, MA: Kluwer, 1999.

Anselmo Barbosa Rodrigues received the first and M.Sc. degrees in electrical engineering from Federal University of Maranhão (UFMA), São Luís, Brazil, in 1998 and 2003, respectively. He is pursuing the Ph.D. degree in electrical engineering at Pontifical Catholic University of Rio de Janeiro, Rio de Janeiro, Brazil.

His primary research interest is reliability assessment in composite and distribution systems.

Ricardo B. Prada was born in 1951. He received the diploma in electrical engineering and the M.Sc. degree in power systems from the Pontifical Catholic University of Rio de Janeiro, Rio de Janeiro, Brazil, in 1975 and 1977, respectively, and the Ph.D. degree in electrical engineering from Imperial College of Science and Technology, London, U.K., in 1980.

He is an Associate Professor in the Department of Electrical Engineering, Pontifical Catholic University of Rio de Janeiro, Rio de Janeiro, Brazil.

Maria Da Guia da Silva (M'99) received the B.Sc. and M.Sc. degrees in power engineering from Federal University of Paraiba, Paraiba, Brazil, in 1980 and 1986, respectively, and the Ph.D. degree in power engineering from the University of Manchester Institute of Science and Technology, Manchester, U.K., in 1994.

She is an Associate Professor in the Department of Electrical Engineering, Federal University of Maranhão, São Luís, Brazil. Her primary research interest is the modeling and application of probabilistic techniques for power system problems, particularly those concerned with reliability and power quality.